The Impact of Sunlight on the Performance of Visible Light Communication Systems over the Year

Mahmoud Beshr
Strathclyde Univeristy
Glasgow,UK

Ivan Andonovic
Strathclyde Univeristy
Glasgow,UK

Moustafa Hussien
Arab Academy for Science and Technology
Alexandria,Egypt

Abstract

Visible light communications (VLC) is a valuable addition to future generations of networks, utilizing light for illumination for the purposes of advanced service provisioning at high speed. Low energy consumption, license free and RF interference free operation are compelling advantages. VLC systems are affected by sunlight limiting connection availability and reliability. The paper presents an analysis of the performance of VLC systems at different locations around the world over the cycle of a year; the evaluation considers the impact of sunlight as a function of location, time and for different surfaces over the four seasons of the year.

Keywords:

Visible light communications, Availability, Sunlight intensity, Performance analysis.

Introduction

VLC is a high-speed, secure, energy efficient network using very large bandwidth pulsed light instead of radio waves or microwaves, providing a relatively high data rate and interference free operation within application environments where issues with RF interference are a fundamental barrier [6].

VLC is impacted by sunlight intensity, the latter depending on location, day of the year, time of day and meteorological condition. 47% of the sunlight spectrum lies within the visible light frequency band, the band of network operation. To date the evaluation of the performance of VLC systems has not rigorously considered the impact of sunlight [1], [2], [4]. In previous research, sunlight has been treated as Gaussian noise; this research takes into consideration the variation of sunlight intensity over the year of 2011. Hourly sunlight irradiance for two representative hospital environments, Cairo, Egypt and Glasgow, Scotland are considered and the calculation of solar irradiance, considers the longitude and latitude of locations, day of year and time of day.

The VLC impulse response has to date been determined solely for single reflection for standard room sizes [2], [4]. Here an evaluation of the impulse response for relatively large room sizes for both line-of-sight (LOS) and non-line-of-sight (NLOS) components up to the fifth reflection is presented.

The paper is organized as follows. Section one presents the VLC system architecture and its mathematical representation. Section two summarizes the foundation for the treatment of the impact of sunlight and its mathematical representation. Section three presents VLC system performance considering the impact of natural light and Section four draws conclusions.

Unmanned/Unattended Sensors and Sensor Networks IX, edited by Edward M. Carapezza,
Proc. of SPIE Vol. 8540, 85400F · © 2012 SPIE · CCC code: 0277-786/12/$18 · doi: 10.1117/12.978935

System Model

It is assumed that the optical path is subject to multiple refections [2] (Fig.1) andthat the transmitter is positioned on the ceiling of the room with the receiver on the floor. Transmitter radiated light is characterised by Φ_1 , equal to the viewing angle of the LED. The beam is incident with angle θ_1 after distance *d* from source to reflection point.

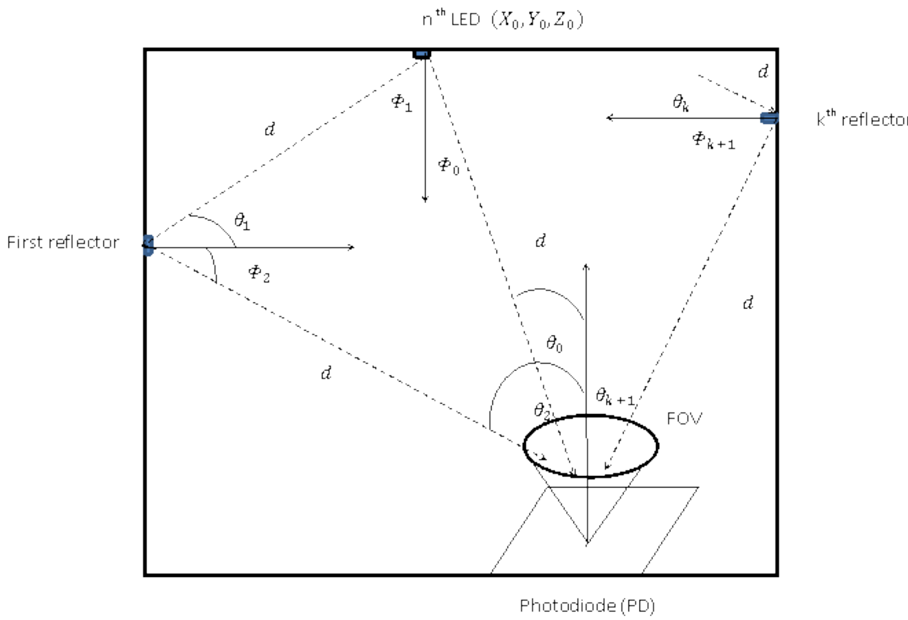

Fig.1. Geometry of the analysis environment comprising n transmitter LEDs and a receiver photodiode (PD).

Link geometry of Fig.1 is considered in order to calculate the impulse response for the case of multiple reflections and multiple sources. The impulse response is given by Equation (1), where N_{LED} is the total number of LEDs. It is assumed that each LED in the transmitter emits equal power. The response after k-reflections of the n^{Th} LED is [2], [3], and [7]:

$$h(t) = \sum_{n=1}^{N_{LED}} \sum_{k=0}^{\infty} h^{(k)}(t; \Phi_n) \tag{1}$$

$$h^{(k)}(t;\Phi_n) = \int_s \left[L_1 L_2 \dots\dots L_{K+1} \Gamma_n{}^{(k)} rect(\frac{\theta_{k+1}}{FOV}) \times \delta(t - \frac{d_1 + d_2 + \cdots d_{k+1}}{c} \right] dA_{ref},\ k \geq 1 \tag{2}$$

where

$$L_1 = \frac{A_{ref}(m+1)cos^m \Phi_1 cos\theta_1}{2\pi {d_1}^2}$$

$$L_2 = \frac{A_{ref} \cos \Phi_2 cos\theta_2}{\pi {d_2}^2}$$

$$L_{k+1} = \frac{A_{PD} \cos \Phi_{k+1} \cos \theta_{k+1}}{\pi {d_{k+1}}^2}$$

L_{k+1} represent the loss terms for each path. The integration in Equation (2) is performed with respect to the surface $\mathcal{S}$ of all reflectors, and $\mathcal{A}_{\text{ref}}$ is the area of the reflecting element. The mode number of a radiation lobe, $m = -1/\log 2 (\cos \phi_{1/2})$ is a measure of the directivity of the beam and is related to the viewing angle ($2\phi_{1/2}$) of an LED.

The angles of irradiance and incidence are designated as ϕk and θk respectively. Received power is inversely proportional to the square of the distance dk, the distance between source and destination (Fig.1). The photodiode (PD) detects with an angle of incidence less than field of view (*FOV)*; the latter is the acceptance angle of the detector. The rectangular function rect (x) is given by [2], [5].

$$rect(x) = \begin{cases} 1 & for\ |x| \leq 1 \\ 0 & for\ |x| > 1 \end{cases} \tag{3}$$

where the constant term, *c* is the speed of light.

$\Gamma_n^{(k)}$in Equation (2) denotes the power of the reflected ray after k- bounces from the n^{th} LED. The reflected power can be calculated as:

$$\Gamma_n^{(k)} = \int_\lambda \Phi_n(\lambda)\,\rho_1(\lambda)\rho_2(\lambda)\ldots\ldots\rho_k(\lambda)d\lambda \tag{4}$$

The reduced form of Equation (4) (with lower accuracy) is:

$$\bar{\Gamma}_n^{(k)} = P_n\bar{\rho}_{n,1}\bar{\rho}_{n,2}\ldots\ldots\ldots..\bar{\rho}_{n,k} \tag{5}$$

where $\bar{\rho}_{n,k} = \frac{1}{P_n}\int_\lambda \Phi_n(\lambda)\rho_k(\lambda)d\lambda$ is the average reflectance, and $P_n = \int_\lambda \Phi_n(\lambda)d\lambda$ is the radiant power from the n^{th} LED source for *k*=1. Equations (4) and Equation (5) have the same value [2]:

$$\Gamma_n^{(1)} = \bar{\Gamma}_n^{(1)} = \int_\lambda \Phi_n(\lambda)\rho_1(\lambda)d\lambda \tag{6}$$

However, the differences are more obvious for the case of higher order reflections. The photodiode position for LOS is given as [2], [7]:

$$h^{(0)}(t;\Phi_n) = L_O P_n rect(\frac{\theta_o}{FOV})\delta(t - \frac{d_o}{c}) \tag{7}$$

where

$$L_O = \frac{A_{PD}(m+1)cos^m\Phi_o cos\theta_o}{2\pi{d_0}^2}$$

Signal-to-Noise Ratio (SNR)

In order to determine the SNR and concomitant Bit Error Rate (BER), it is assumed that the transmitter sends data at a bit rate R_b using ON-OFF keying (OOK) with NRZ pulses. The transmitted average power is P_t, the received average power is $p = H(0)P_t$, where the channel DC gain is determined as detailed in the previous section. The channel is assumed to be distortion free with gain H (f) = H (0) for all frequencies. The receiver pre-amplifier is followed by an equalizer. Each sample of the equalizer output contains noise with a total variance given by [2], [3], [7], [8]:

$${\sigma_{total}}^2 = {\sigma_{shot}}^2 + {\sigma_{thermal}}^2 \tag{8}$$

The shot noise is;

$${\sigma_{shot}}^2 = 2qRp_nI_2R_b \tag{9}$$

while the thermal noise variance is given by:

$$\sigma_{thermal}{}^2 = \frac{4KT}{R_F} I_2 R_b + \frac{16\pi^2 KT}{g_m}\left(\Gamma + \frac{1}{g_m R_D}\right) C_T{}^2 I_3 R_B{}^3 + \frac{4\pi^2 K I_D{}^a C_T{}^2}{g_m{}^2} I_f R_b{}^2 \tag{10}$$

The SNR is expressed using Equation (8), Equation (9), and Equation (10);

$$SNR = \frac{(RP)^2}{\sigma_{total}{}^2} \tag{11}$$

and the BER is given by;

$$BER = Q(\sqrt{SNR}) \tag{12}$$

where

$$Q(x) = \frac{1}{\sqrt{2\pi}} \int_x^\infty e^{-y^2/2} dy \tag{13}$$

Sunlight Irradiance

VLC systems are strongly influenced by sunlight irradiance over the day, varying from sunrise to sunset. Incident solar radiation is a function of several variables including the time of day, the day of the year, geographic location, and atmospheric conditions. Direct solar radiation, q_{sun} could be measured at the proposed location through photodiodes. However in the absence of accurate measurements, the sunlight irradiance can be calculated from the approximation of clear sky solar radiation on a horizontal surface in W/m^2 as [1],[9]:

$$q_{sun}^{\backslash} = 1350.3\left[1 + 0.033\cos\left(\frac{360n}{365}\right)\right]\left[\sin\varphi \sin\delta + \cos\varphi \cos\delta \cos\omega\right] \tag{14}$$

where δ is solar declination , ω is the angular displacement and φ is the location longitude. Two corrections in time calculations are used to convert from local clock time into apparent solar time. The first correction takes into consideration the variation in the earth's rate of rotation; the second correction is an adjustment for the difference in local longitude and the standard meridian for the local time zone [1],[9].

The declination, in degrees, is:

$$\delta = 23.45 \sin\left[360\left(\frac{284 + n}{365}\right)\right] \tag{15}$$

The angular displacement of the sun, east or west of the local meridian due to the earth's rotation (afternoon positive) is the angle hour. The angle hour, in degrees, is:

$$\omega = 15(12 - AST) \tag{16}$$

The apparent solar time (AST), is related to the local standard time, (LST), given in minutes from midnight by:

$$AST = LST + E \pm 4(\eta - \psi) \tag{17}$$

In Equation (17), the positive sign is for west, and the negative sign is for east of the Greenwich meridian (zero longitude) where, η is Standard meridian for the local time zone in degrees west of the Greenwich meridian. ψ is the local longitude in degrees east or west of the Greenwich meridian (zero longitude). E is the equation of time, which can be calculated for the day of the year (n) and divided into four main periods [1], [9]:

- Between 1st January and 15th April, (1<= n <=105).

$$E = -14.2\sin[0.028303(n+7)] \tag{18}$$

- Between 16th April and 15th June, (106<= n <=165).

$$E = 4\sin[0.053247(n-106)] \tag{19}$$

- Between 16th June and 31st August, (166 <= n <= 245).

$$E = -6.5\sin[0.03927(n-166)] \tag{20}$$

- Between 1st September and 31st December, (246 <= n <= 365).

$$E = 16.4\sin[0.027802(n-246)] \tag{21}$$

Sunlight irradiance for Cairo and Glasgow is summarized for the four seasons of the year in Table I and Table II respectively.

Table I. Sunlight irradiance in Cairo for year of 2011.

Season of year	Minimum sunlight irradiance (W/m^2)	Maximum sunlight irradiance (W/m^2)
Summer	0.48	1312.911
Autumn	3.280	1175.087
Winter	1.446	1185.579
Easter	1.861	1314.609

Table II. Sunlight irradiance in Glasgow for year of 2011.

Season of year	Minimum sunlight irradiance (W/m^2)	Maximum sunlight irradiance (W/m^2)
Summer	0.598	1114.804
Autumn	1.606	749.22
Winter	1.189	767.309
Easter	0.485	1114.88

System Performance

Signal to Noise Ratio (SNR) was calculated for each season over the year listed in Table III .Monte Carlo simulations together with a Matlab routine were used to model the system, simulate and evaluate the average SNR. The analysis was carried out for a 100 Kbit/s data rate and 0.54 $A/_{W}$ photodiode responsivity.

Winter Season

Figure 2 and Figure 3 show that average SNR for plaster wall, ceiling ,floor and plastic wall surfaces during winter; the effect of sunlight is weak since its intensity is relatively low. The average SNR for plastic walls (lowest reflectivity) is ~19dB in Glasgow and ~ 17dB in Cairo and ~ 36dB and ~33dB for plaster walls (highest reflectivity) for Cairo and Glasgow respectively. For ceiling and floor surfaces the average SNR was ~29dB, ~33dB, ~27.5dB, ~28.5dB for Glasgow and Cairo respectively. The system can provide a 10^{-12} BER for plaster walls, plastic walls and ceilings and 10^{-10} for floor surfaces.

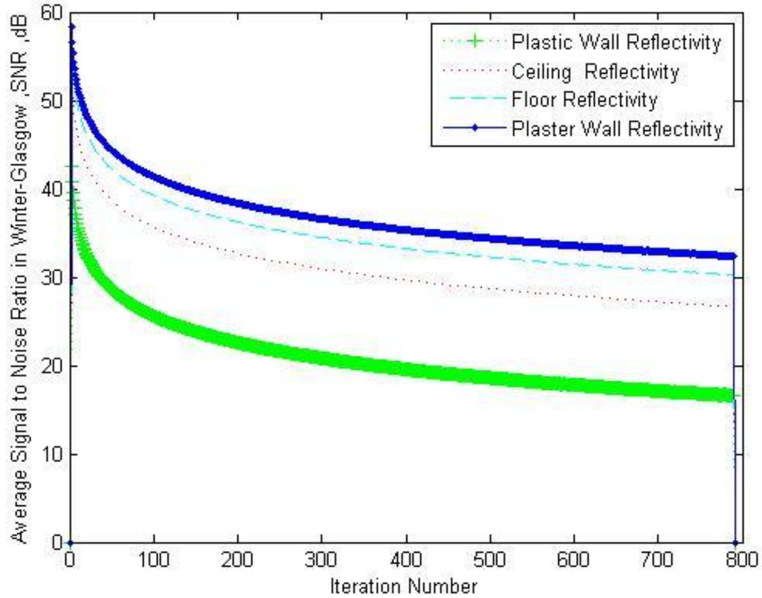

Fig.2. Average SNR in winter, Glasgow.

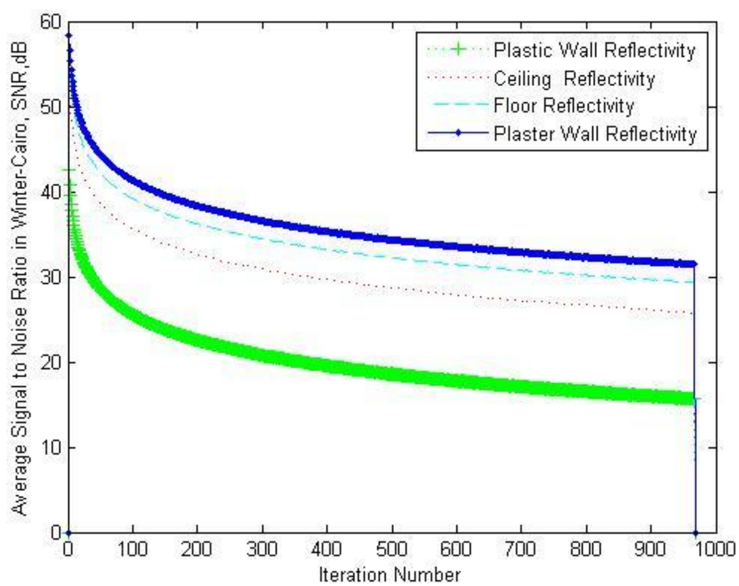

Fig.3. Average SNR in winter, Cairo

Summer season

During the summer season, sunlight intensity increases up to 1175 W/m^2 and the average SNR degrades to ~15dB and ~13.5 dB for plastic wall surfaces and 31dB and 30dB for Glasgow and Cairo respectively (Figure 3, Figure 4). A further decrease in the average SNR for floor and ceiling surfaces is evident but a BER at 10^{-9} is still attainable.

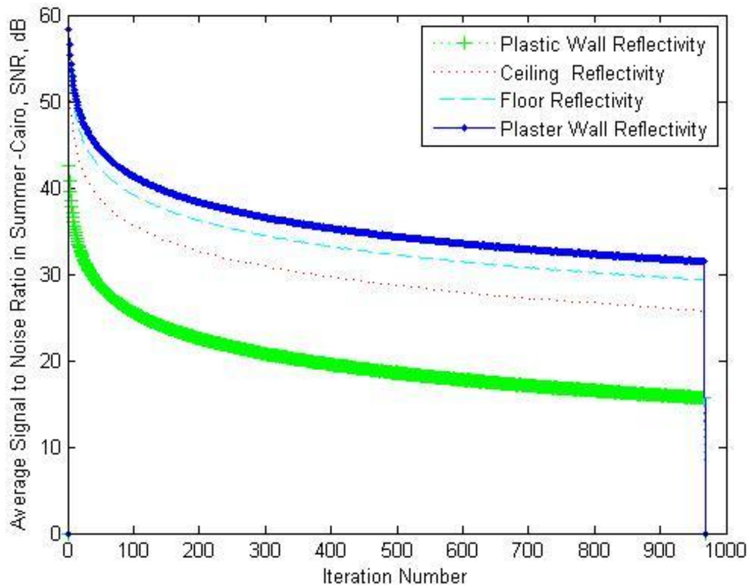

Fig.4. Average SNR in summer, Cairo

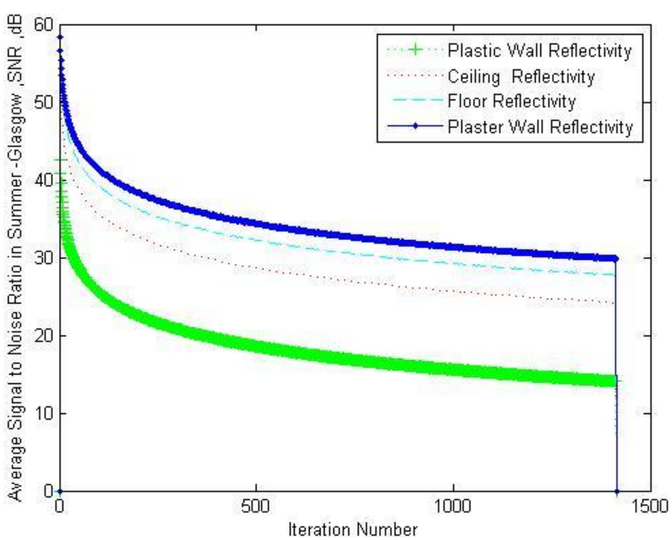

Fig.5. Average SNR in summer, Glasgow.

Autumn Season

As sunlight intensity lowers in the autumn period, the average SNR increases; for plastic walls and plaster walls to ~ 18dB, ~34dB and ~17dB , ~32dB in Glasgow and Cairo respectively. Furthermore, increases in the average SNR to ~28dB, ~27dB and ~33dB, ~30dB in Glasgow and Cairo respectively (Figure 5 and Figure 6) for ceilings and floors are observed. A BER up to 10 $^{-10}$ for plastic walls and ~10 $^{-11}$ for other surfaces is attainable.

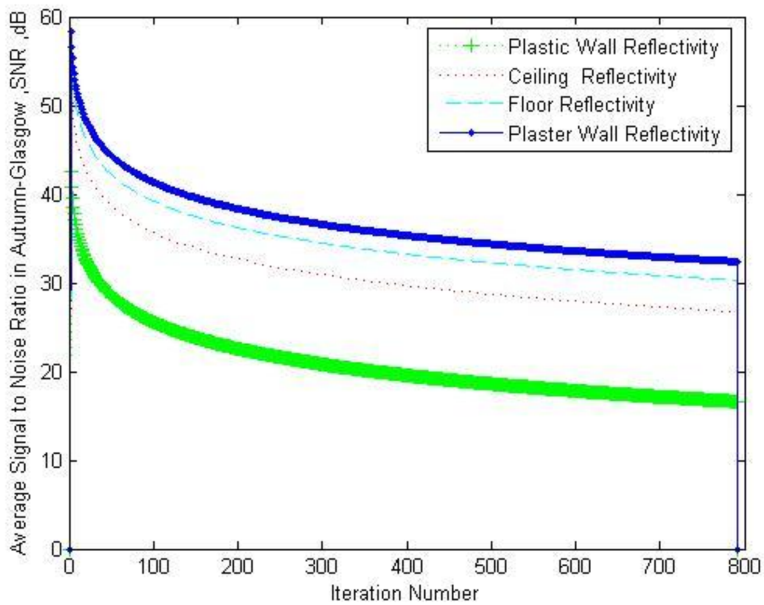

Fig.6. Average SNR in autumn, Glasgow.

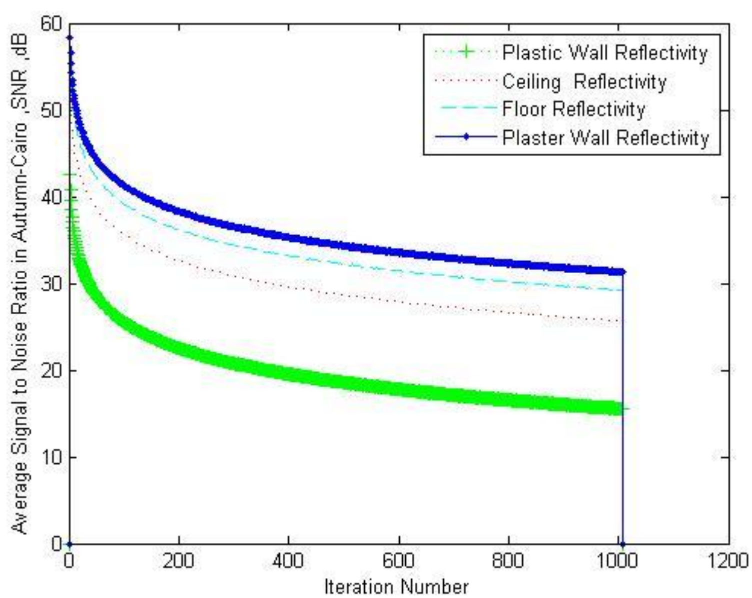

Fig.7. Average SNR in autumn, Cairo

Spring Season

Sunlight intensity increases to 1314 W/m^2 compared to winter in spring and thus the average SNR also increases (Figure 8 and Figure 9). The SNR was ~ 15dB for plastic walls in both Glasgow and Cairo, 25dB, 28dB, 30dB for ceilings, floors and plaster walls in Cairo and ~27dB, ~30dB, ~31dB in Glasgow. Moreover the BER level ranges from 10^{-10} for plastic walls, 10^{-11} for ceilings and 10^{-12} for both floors and plaster walls.

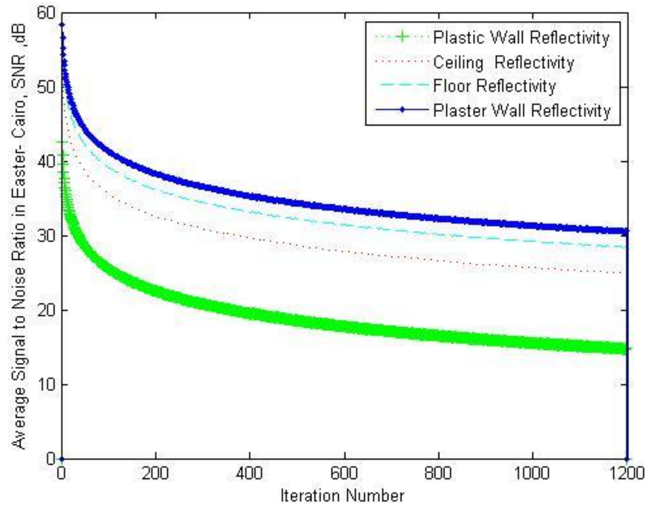

Fig.8. Average SNR in spring, Cairo.

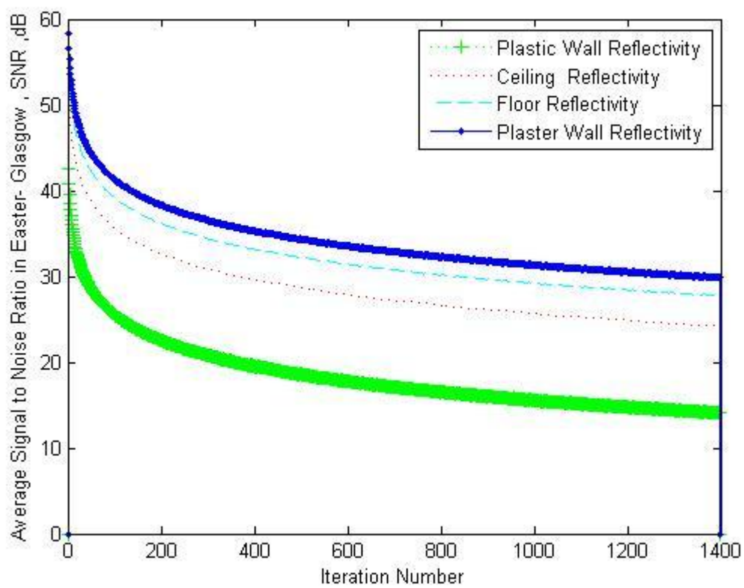

Fig.9. Average SNR in spring, Glasgow.

Conclusions

The impact of sunlight irradiance on VLC system performance was evaluated for summer, spring, autumn, and winter seasons of year 2011 (Table III). The evaluation considered the achievable BER for the four seasons of year for a range of surfaces; plaster walls, floors, plastic walls and ceilings; the attainable BER ranges from 10^{-9} to 10^{-12}. All simulations were conducted using hourly calculations (8760 hours) of sunlight irradiance and it was found that the lowest SNR (and BER) occurred for summer days in Cairo where sunlight intensity reaches its maximum. Further research on the effects of on the sunlight intensity will be considered.

Table III .Summary of SNR over the four seasons of year.

SNR / Season	Plaster wall (dB)		Floor (dB)		Ceiling(dB)		Plastic wall (dB)	
	Cairo	Glasgow	Cairo	Glasgow	Cairo	Glasgow	Cairo	Glasgow
Summer	~ 30	~ 31	~ 29	~ 27.5	~ 23.5	~ 25	~13.5	~ 15
Autumn	~ 32	~ 34	~ 30	~ 33	~.27	~ 28.5	~ 17	~ 18
Winter	~ 33	~ 36	~ 28.5	~ 33	~ 27.5	~ 29	~ 17	~ 19
Spring	~ 30	~ 31	~ 28	~ 30	~ 25	~ 27	~ 14	~ 14.5

In summary, the availability of VLC systems is a strong function of the level of natural sunlight and indeed the performance may be compromised under high intensity scenarios such as encountered during summer periods.

References

[1] J. Duffie, and W. Beckman, “Solar Engineering of Thermal Process”, 2nd Ed., N. Y. John Wiley & Sons, 1991.

[2] Kwonhyung, L.; Hyuncheol, P.and Barry, J.R., "Indoor Channel Characteristics for Visible Light Communications," Communications Letters, IEEE, vol.15, no.2, pp.217-219, February 2011.

[3] Gfeller, F.R., Bapst, U., "Wireless in-house data communication via diffuse infrared radiation," Proceedings of the IEEE, Vol.67, no.11, pp. 1474- 1486, Nov. 1979.

[4] Lubin Z.; Minh H.L., O'Brien, D., Faulkner, G.; Kyungwoo L.,Daekwang J.andYunJe Oh., , "Equalisation for high-speed Visible Light Communications using white-LEDs," Communication Systems, Networks and Digital Signal Processing, 2008. CNSDSP 2008. 6th International Symposium, pp.170-173, 25-25 July 2008.

[5] Barry, J.R., Kahn, J.M., Krause, W.J., Lee, E.A.and Messerschmitt, D.G., "Simulation of multipath impulse response for indoor wireless optical channels," Selected Areas in Communications, IEEE Journal on , Vol.11, No.3, pp.367-379, Apr 1993.

[6] Komine, T., Nakagawa, M., "Fundamental analysis for visible-light communication system using LED lights," Consumer Electronics, IEEE Transactions, Vol.50, No.1, pp. 100- 107, Feb 2004.

[7] Kahn, J.M.; Barry, J.R.; "Wireless infrared communications," Proceedings of the IEEE, vol.85, no.2, pp.265-298, Feb 1997.

[8] Ramirez, R.; Idrus, S. and Johor, S.; Optical wireless communications IR for wireless connectivity, CRC press, Taylor & Francis, 2008.

[9] Quaschning, V., Understanding Renewable Energy Systems, Earthscan, United Kingdom, 44-62(2005).